Simulation of photovoltaic grid connected inverter in case of grid-failure

Aissa Chouder[1, 2,*] , Santiago Silvestre [1] and Ali Malek [2]

[1] Electronic Engineering Department, Universidad Politècnica de Cataluña,
Mòdul C4, Campus Nord UPC, Gran Capitán s/n, 08034 Barcelona, Spain

[2] PV Solar Energy Division, Centre de Développement des Energies Renouvelables,
B.P. 62, Route de l'Observatoire, Bouzaréah, Algiers, Algeria

Abstract - *In this paper, a behavioural model of photovoltaic grid connected system is presented and simulated. The photovoltaic generator and a single phase inverter are modelled both by the well known one diode model and a current controlled voltage source respectively. The indirect current control method has been applied to achieve the inverter current control in order to feed a sinusoidal current waveform to the ac grid. Finally, normal and faulty conditions of the photovoltaic generation, especially in the case of grid failure, were simulated and commented.*

Résumé - *Dans cet article, un modèle comportemental d'un système photovoltaïque connecté au réseau est présenté et simulé. Le générateur photovoltaïque et un onduleur monophasé sont modélisés respectivement à l'aide du modèle bien connu à une diode, et d'une source de courant contrôlée en tension. La méthode de contrôle du courant indirect a été appliquée pour la commande du courant de l'onduleur afin d'injecter une onde de courant sinusoïdal au réseau alternatif. En conclusion, des conditions normales et défectueuses de la production photovoltaïque, particulièrement dans le cas d'un problème de réseau, ont été simulés et commentés.*

Key words: PV generator - Inverter - Control strategies - Grid-failure - Pspice.

1. INTRODUCTION

As the conventional energy sources are dwindling fast, the solar photovoltaic energy offers a very promising alternative, because it is free, abundant, pollution free and distributed throughout the earth. In the past, photovoltaic energy has been used as power supply for only some loads such as satellites or remote areas where conventional sources are very far.

In these days of increasing environmental concern, governments and the scientific community work to maximize the use of renewable energy resources. There is a growing recognition of the valuable role solar power can play in reducing pollution, particularly in the effort to stabilize the carbon dioxide levels. The technology is now available for industrial, commercial and residential consumers. Photovoltaic (PV) power supplied to the utility grid is gaining more and more visibility due to many national incentives [1].

With a continuous reduction in system cost (PV modules, DC/AC inverters, and installation), the PV technology has the potential to becomes one of the main renewable energy sources for the future electricity supply. The market for grid-connected PV power applications continues to develop at a high rate.

Feeding the photovoltaic energy to the ac grid is not evident. It poses some problems in controlling the energy transfer and connecting the two systems together by using static converters.

The classical connection between photovoltaic array and AC grid is shown in figure 1. The main objective, from this interfacing, is to feed all the collected energy at the PV plant to the commercial AC grid.
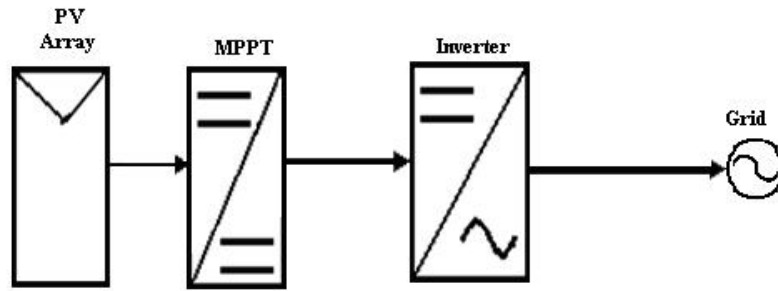
---

* chouder@eel.upc.edu

Fig. 1: PV grid connected system

This is achieved by the followings:

- PV array wish is responsible to transform the sun light to electricity.
- MPPT controller, this is used to maximise the power coming from PV array at any atmospheric conditions.
- Inverter, this is a device witch transform DC input to an AC output at the same waveforms as the grid line.

2. MODELING AND SIMULATION OF THE PV GRID SYSTEM

2.1 Characteristics of PV array

Basically, PV cell is a P-N semiconductor junction that directly converts light energy into electricity. It has the equivalent circuit shown in figure 2 [2].
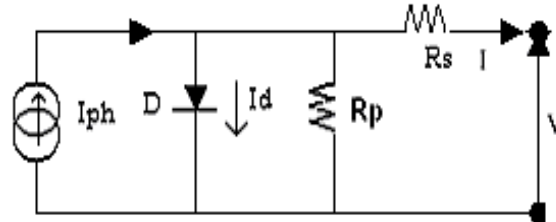
Fig. 2: Equivalent PV cell circuit

The current source I_{ph} represents the cell photocurrent; R_s and R_p are the intrinsic serie and shunt resistance of the cell respectively. The PV cell exhibit a non-linear voltage-current characteristics. The followings are the simplified equations describing the behaviour of the PV cell [3].

$$I = N_p I_{ph} - N_p I_{sat} \left(\exp \frac{q V / N_s}{A k T_c} - 1 \right) \tag{1}$$

$$I_{ph} = \left\{ I_{sc} . \phi_N + I_t \left(T_c - T_r \right) \right\} . N_p \tag{2}$$

$$I_{sat} = I_{or} \left(\frac{T_c}{T_r} \right)^3 . e^{\frac{q E_g}{B k} \left(\frac{1}{T_r} - \frac{1}{T_c} \right)} \tag{3}$$

$$V_{oc} = \frac{k T_c}{q} . \ln \left[\frac{I_{sc}}{I_{sat}} + 1 \right] \tag{4}$$

Where I is the PV array output current; V is the PV array output voltage; q is the charge of an electron; k is Boltzman's constant; E_g is the band gap of the semi conductor; I_{sat} is the diode reverse saturation current; T_c and T_r are the cell temperature and the reference temperature both in Kelvin; A and B are the diode ideality factors where their values varied between 1 and 2; Φ_N is the normalized insolation; I_{sc} is short circuit current given at standard condition; I_t and I_{or} are constants given at standard conditions; N_s and N_p are the serie and parallel cell number respectively.

Figure 3 shows the $I-V$ characteristics at different insulation levels (*Module Isofoton 106-12, $N_s = 36$, $N_p = 2$*).
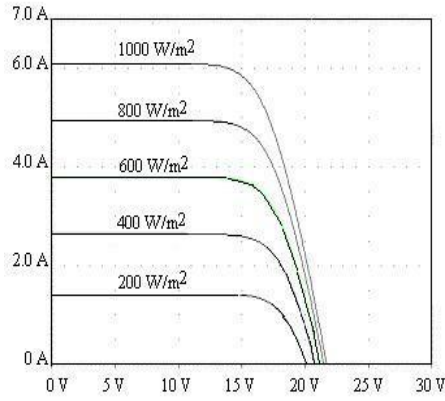
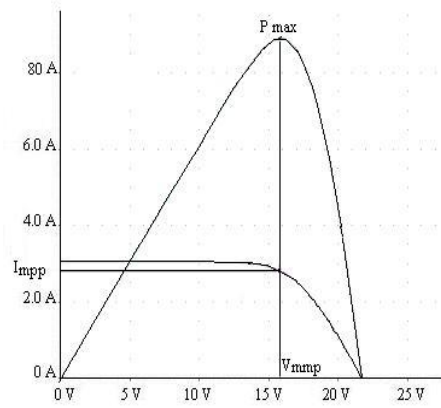Fig. 3: I-V characteristics of PV panel   Fig. 4: P-V characteristics of PV panel

It is shown, in those figures, that the maximum power that can be delivered by a PV panel depends greatly on the insulation level and the operating temperature. Therefore, it is necessary to track the maximum power point all the time. Many researches have been focused on various MPP control algorithm to lead the operating point of the PV panel to optimum point. Among of them, the constant voltage method, the perturbation and observation (P&O) method and incremental conductance method (IncCond) [4].

2.2 Maximum power point derivation

In order to get the shape of the injected current to the grid, it is necessary to calculate the coordinates of the maximal power point (V_{mpp}, I_{mpp}). For this, and to simplify the implementation model in Pspice, the coordinates of the maximum power point are given by the following equations [5]

$$I_{mpp} = I_{ph} - I_{sat} \cdot \left(e^{V_{mpp} / V_t} - 1 \right) \tag{5}$$

$$V_{mpp} = V_t \ln \left(1 + \frac{I_{ph} - I_{mpp}}{I_{ph}} \left(e^{V_{oc} / V_t} - 1 \right) \right) \tag{6}$$

where V_t is the thermal voltage given by:

$$V_t = \frac{k\,T_c}{q} \tag{7}$$

The simulations results of 3 kW$_p$ photovoltaic grid connected system are shown in the figures below. The entry to the simulation file is a real data of solar insulation and temperature in one day.
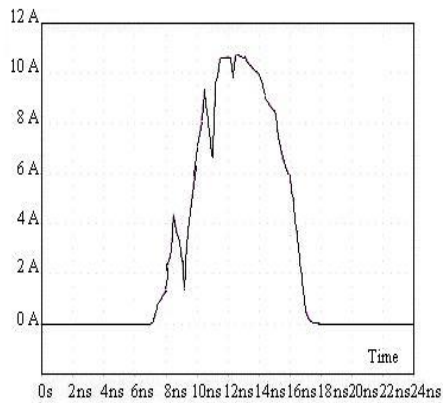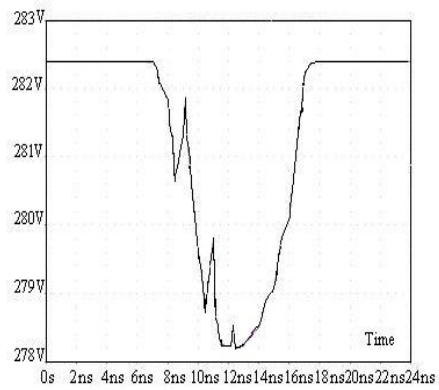

Fig. 5: Simulated optimal current, I$_{mpp}$
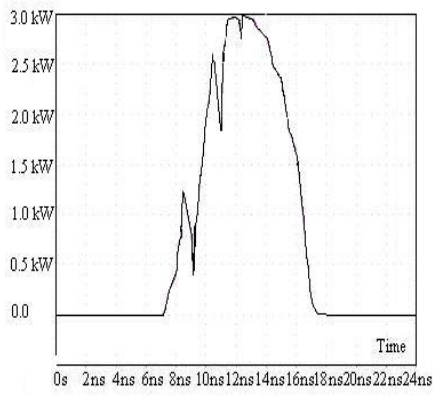

Fig. 6: Simulated optimal voltage, V$_{mpp}$
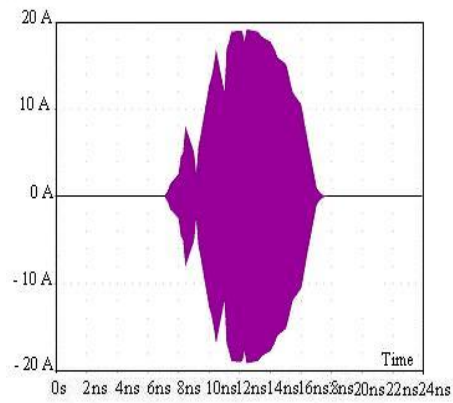

Fig. 7: Simulated maximum PV power, P max

Fig. 8: Simulated shape of the grid injected current, I$_{grid}$

2.3 Inverter modelling

The main spefication of the grid connected inverter is that current must be drawn from the PV plant and delivered to the utility grid at unity power factor [6].

Consider the grid connected inverter of figure 9 where:
- Vinv : Fundamental component of inverter output
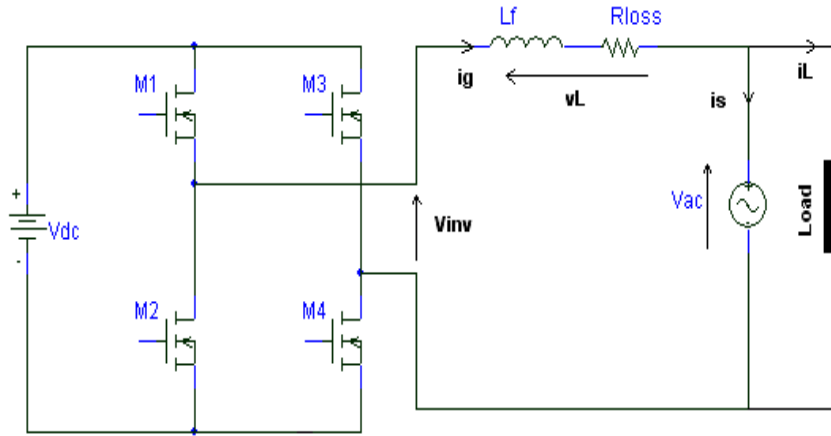- vL : Voltage drop across the link inductor
- Vac : Utility grid waveform.

Fig. 9: Full bridge grid connection

Assuming that the losses are negligible, It is seen that:

$$V_{inv} = V_{ac} + vL \tag{8}$$

Where all variables are vectors of the form: $v = V e^{j\varphi}$

Then:

$$V_{inv} = V_{ac} + j . L_f . \omega . I_g \tag{9}$$

To achieve the unity power factor condition, the current waveform must be in phase from the utility voltage waveform, in vector form this looks like:

The key to controlling this operation is the inverter voltage variable, V_{inv}. From equation (9), I_g can be written as:

$$I_g = \frac{V_{inv} - V_{ac}}{j \omega L_f} \tag{10}$$
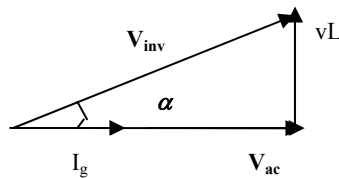
Drawn as phasor, this looks like:

Fig. 10: Magnitude and phase requirement

The above phasor in figure 10 shows that the magnitude and direction of current flow (and therefore power flow) can be controlled by the phase shift α and magnitude of the inverter output waveform.

2.4 Simulation of the PV grid inverter

Due to the high computational requirement of a full PWM implementation, a simplification has been made to the inverter model. The full bridge inverter is modelled as current controlled voltage source, where harmonic content is ignored. In this case an indirect current control is used to draw a reference current given by the calculated maximum power from the PV model.

The magnitude of the current that the inverter has to draw is given by the power balancing principles:

$$I_g = \frac{\sqrt{2} \cdot I_{mpp} \cdot V_{mpp} \cdot \eta}{V_{aceff}} \tag{11}$$

where η is the inverter efficiency, assumed to be constant ($\eta = 0.95$).

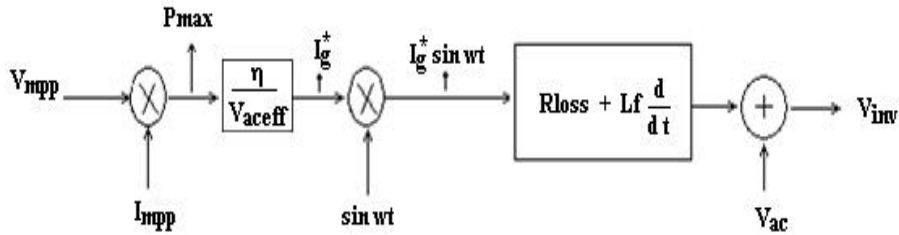The control bloc diagram of the inverter voltage is given in the figure below.

Fig. 11: Bloc diagram of the control system

The implementation of this bloc diagram in Pspice is shown in figure 12. In this scheme, an Average Behaviour Modelling (ABM) is used. The inverter output is modelled as a voltage controlled voltage source. The reference current that must be feeded to the utility is calculated from the PV model and is modelled as current controlled current source.
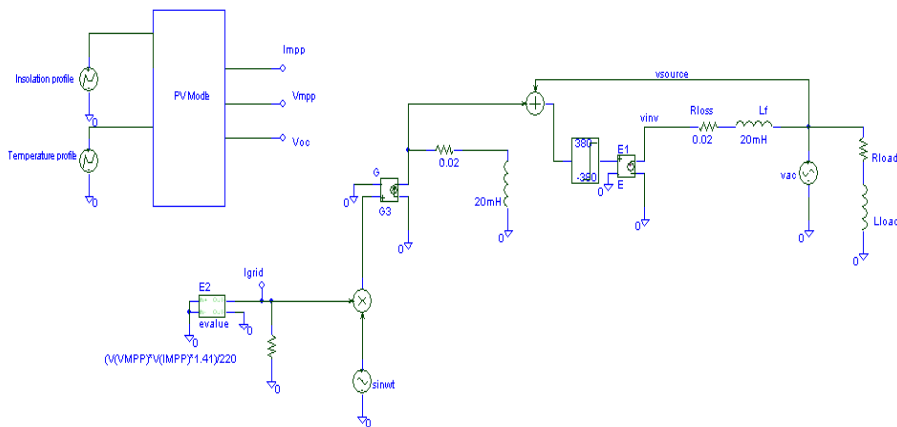

Fig. 12: Pspice schematic of PV grid connected inverter

2.5 Simulation results

Case 1: Simulation results with a constant insolation

The simulations has been carried out with the following parameters:

$\Phi = 600 \text{W} / \text{m}^2$, Load power factor ($\cos \varphi = 0.85$), $L_{load} = 20$ mH , $R_{load} = 10 \, \Omega$.

The inverter parameters are:

$L_f = 20$ mH , $R_{loss} = 0.02 \, \Omega$.
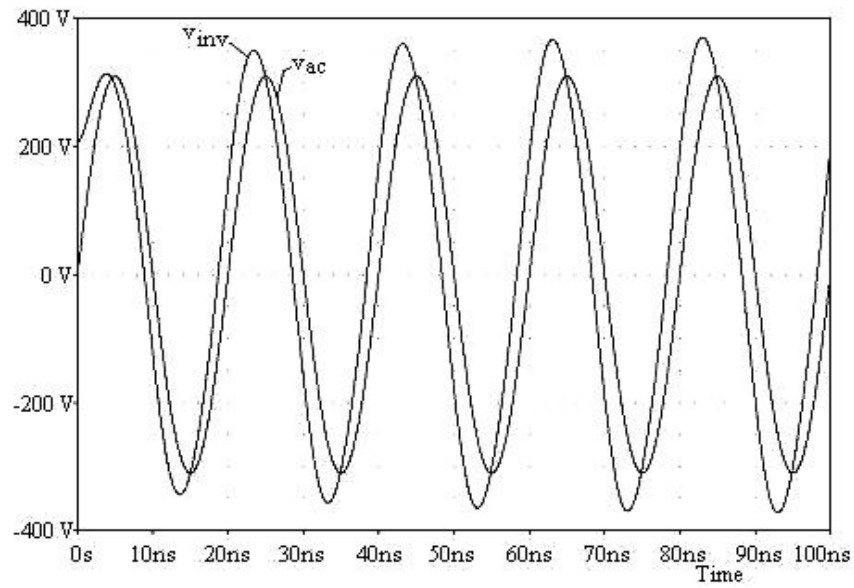
The simulation results are shown in the figures below.

Fig. 13: Simulated inverter voltage ' v_{inv} ' vs grid voltage ' v_{ac} '
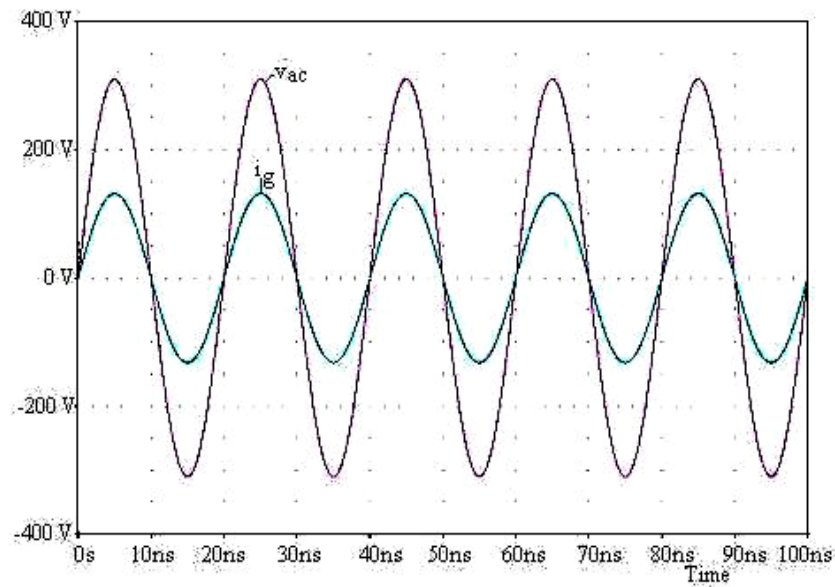

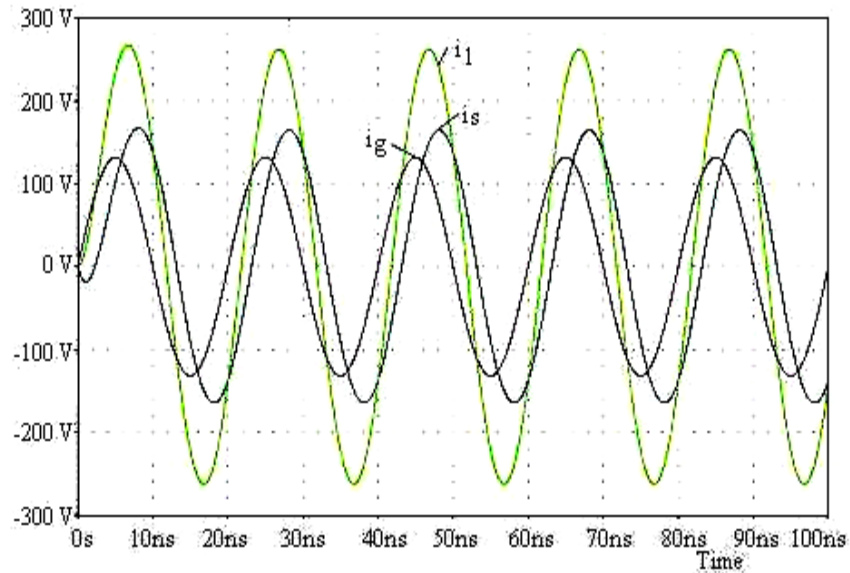Fig. 14: Simulated inverter current ' I_g ' vs grid voltage ' v_{ac} '

Fig. 15: Simulated load current ' I_l ', inverter current ' I_g ' and source current ' I_s '

It is shown in figure 15 that the load current is higher than the grid current, so the remaining amount of current is feeded by the utility grid.

Case 2: <u>Simulation results with a variable insolation</u>

The simulations has been carried out with the following parameters:

Φ variable , Load power factor $\cos \varphi = 0.98$, $L_{load} = 20$ mH , $R_{load} = 100 \ \Omega$.

The inverter parameters are:

$L_f = 20$ mH , $R_{loss} = 0.02 \ \Omega$.

In the case the insolation has been simulated to have a step change as shown in the figure 16.
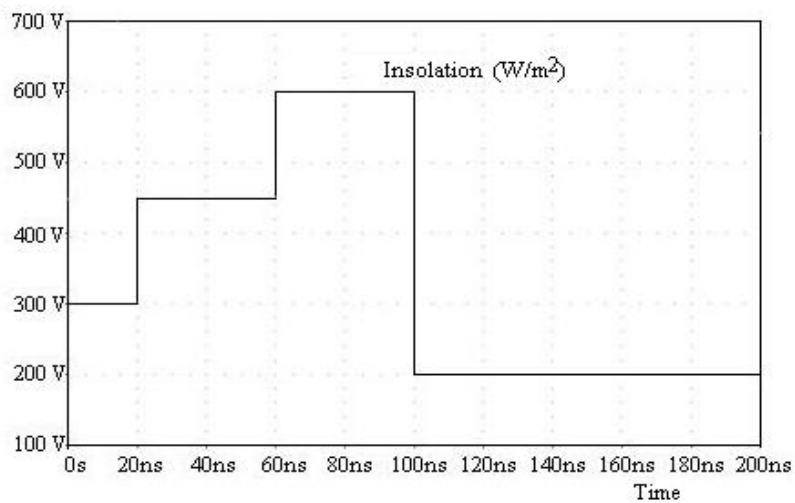

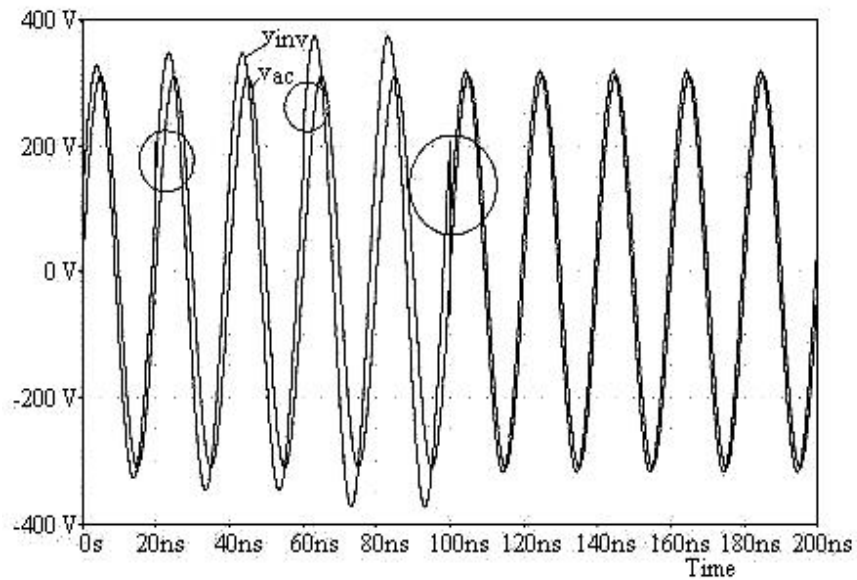Fig. 16: Waveform of the solar insolation

Fig. 17: Simulated inverter voltage ' v_{inv} ' vs grid voltage ' V_{ac} '
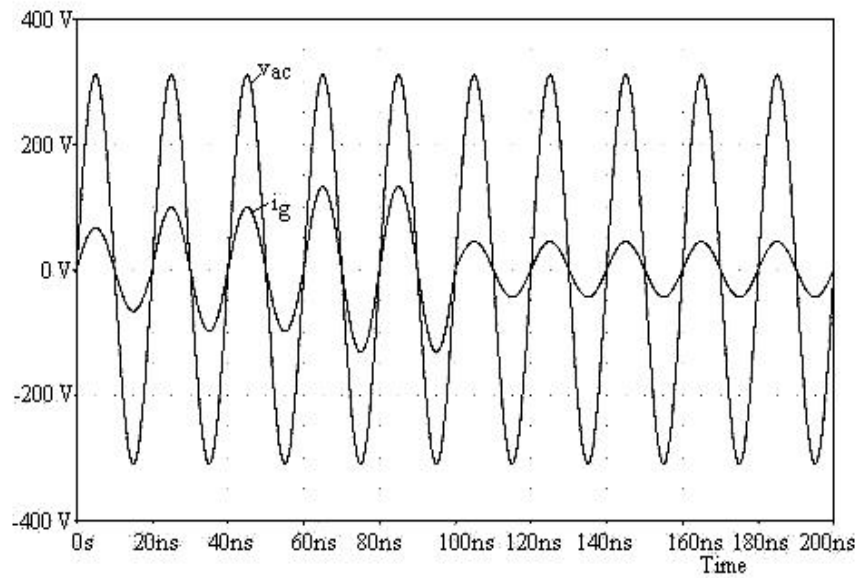

Fig. 18: Simulated inverter current ' I_g ' vs grid voltage ' v_{ac} '

From these waveforms, we notice the sensitivity of the inverter voltage to sudden variations of the reference current. These transitions are accompanied by flickers in the inverter output voltage (Fig. 17). On the other hand, the grid current has a smooth transition due the integration effect of the link inductance. The current load, in this case is smaller than the inverter current. Therefore the remaining current is directly feeded into the grid (Fig. 19).
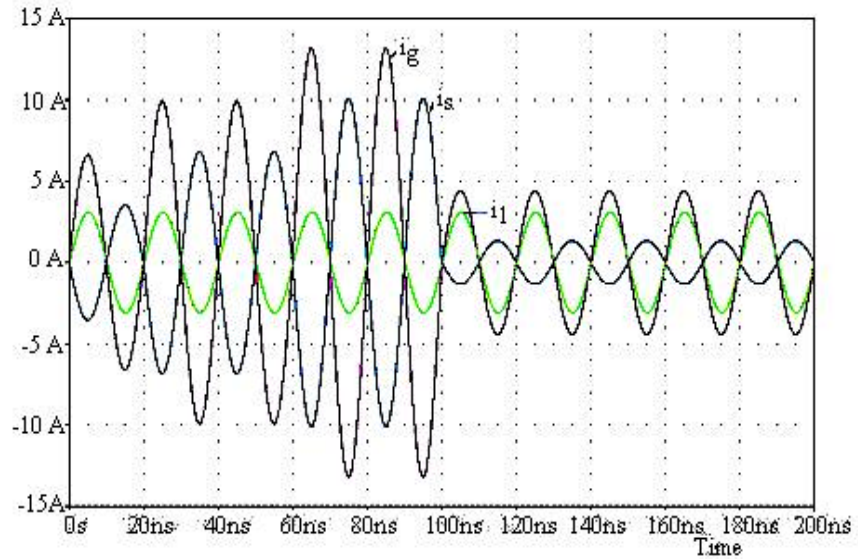
Fig. 19: Simulated inverter current ' I_g ', source current ' I_s ' and load current ' I_l '

Case 3: Simulation results with a grid failure

In this case we investigate the failure case of the grid. The simulations has been carried out with the following parameters:

Instant of grid failure t = 45 ms

$\Phi = 600\,\text{W}/\text{m}^2$, Load power factor $\cos \varphi = 0.98$, $L_{load} = 20$ mH , $R_{load} = 100\,\Omega$.

The inverter parameters are: $L_f = 20$ mH , $R_{loss} = 0.02\,\Omega$.
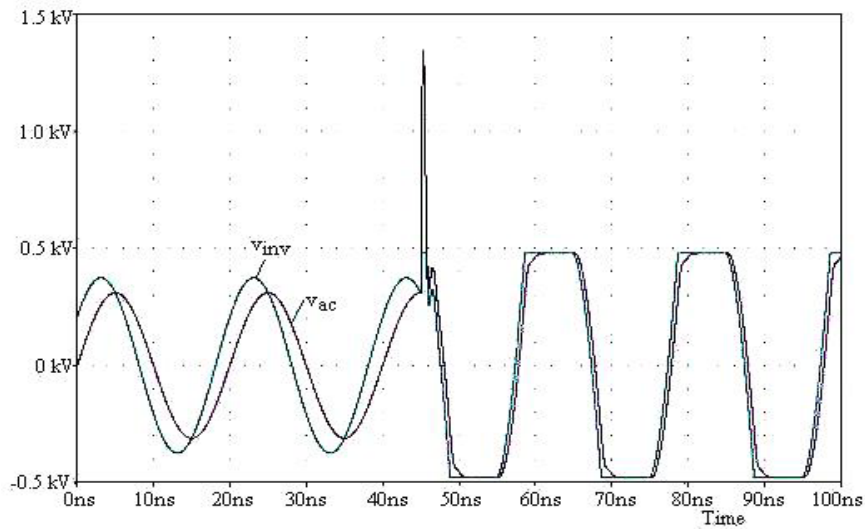
The simulation results are shown in figure 20, 21.

Fig. 20: Simulated inverter output voltage ' V_{inv} ' vs grid voltage ' V_{ac} ' in case of grid failure
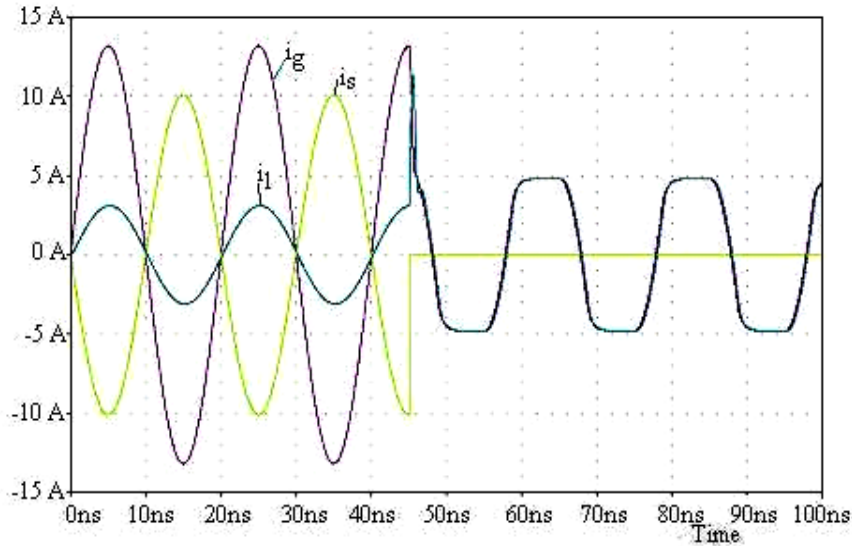
Fig. 21: Simulated inverter output current ' I_g ', source current ' I_s '

and load current ' I_l ' in case of grid failure

From figure 20, we note the apparition of a flicker with a high voltage at the moment of the grid failure, which can cause damages to the connected loads. We note also, the continuous rise of an inverter output voltage until it becomes a square wave due to the limiter effect. This situation is not tolerable in such applications and the inverter control system must detect this state and disconnect the power stage from the line. The same alteration is seen on the current waveforms (Fig. 21) at the grid failure instant. A short time current pic appears in the load current which can cause damage. The load current becomes, after failure, a casi square wave with high harmonic content.

3. CONCLUSION

In this work we presented a simulation study of PV grid connected inverter based on the behavioural model. The indirect current control method has been used to control the inverter output voltage. Three case studies are carried out to see the behaviour of the inverter under different conditions.

The simulation results have shown that the inverter output voltage is sensitive to suden change in the reference current and the ac main voltage failure. Also, the control method used here, requires the knowledge of accurate values of the resistive losses and the filter inductance. But there are inaccuracies in the evaluation the losses parameters in the power switches and the windings of the inductance which make it's implementation very hard to the references current.

REFERENCES

[1] N. Mori, '*Current Status and Future Prospect of Photovoltaic Technologies in Japan*', Proceedings of the 28th Photovoltaic Specialists Conference, Anchorage, Alaska, USA, pp. 1730 - 1733, 2000.

[2] T.F. El Shatter and M.T. El Hagry, '*Sensitivity Analysis of the Photovoltaic Model Parameters*', IEEE, Cir. and Syst., Vol. 2, pp. 914 – 917, 8-11 Aug. 1999.

[3] G.A Gow and C.D. Manning, '*Development of Photovoltaic Model for Use in Power-Electronics Simulation Studies*', IEE, Proceedings of Power Appl., Vol. 146, N°2, pp. 193 – 200, March 1999.

[4] G.J. Yu; Y.S. Jung, J.Y. Choi, I. Choy, J.H. Song and G.S. Kim; '*A Novel Two-Mode MPPT Control Algorithm Based on Comparative Study of Existing Algorithms*', IEEE, Phot. Spec. Conf., pp. 1531 – 1534, 19-24 May 2000.

[5] L. Castañer and S. Santiago, '*Modelling Photovoltaic Systems Using Pspice*', Ed. J. Wiley, 2002.

[6] H. Sugimoto and H. Dong, '*A New Scheme for Maximum Photovoltaic Power Tracking Control*', IEEE, Power Conv. Conf., Vol. 2, pp. 691 – 696 3-6 Aug. 1997.